Morphological Transformations of Native Petroleum Emulsions. I. Viscosity Studies

Igor N. Evdokimov,* Yaroslav O. Efimov, Aleksandr P. Losev, and Mikhail A. Novikov

Department of Physics, Gubkin Russian State University of Oil and Gas, Leninsky Prospekt 65, Moscow B-296, GSP-1, 119991, Russia

Received February 27, 2008. Revised Manuscript Received March 31, 2008

Emulsions of water in as-recovered native crude oils of diverse geographical origin evidently possess some common morphological features. At low volume fractions ϕ of water, the viscosity behavior of emulsions is governed by the presence of flocculated clusters of water droplets, whereas characteristic tight gels, composed of visually monodisperse small droplets, are responsible for the viscosity anomaly at $\phi \approx 0.4-0.5$. Once formed, small-droplet gel domains apparently retain their structural integrity at higher ϕ, incorporating/stabilizing new portions of water as larger-sized droplets. The maximum hold-up of disperse water evidently is the close-packing limit of $\phi \approx 0.74$. At higher water contents (up to $\phi \approx 0.83$), no inversion to O/W morphology takes place, but additional water emerges as a separate phase. The onset of stratified flow (W/O emulsion gel + free water) is the cause of the observed viscosity decrease, contrary to the conventional interpretation of the viscosity maximum as a reliable indicator of the emulsion inversion point.

1. Introduction

The production of crude oil emulsions during petroleum recovery is a ubiquitous and increasingly problematic phenomenon in the oil industry. The resolution of such systems can be a technical and financial burden to the industry as a whole, resulting in reduced production time, operating/processing problems, and heavy costs incurred though the application of a combination of mechanical/chemical/electrical treatment programs. Petroleum emulsions readily form from water/oil mixtures in turbulent flows or because of pressure gradients in reservoir pores, in the chokes at the wellheads and in various valves in piping used for oil production.

A good knowledge of native petroleum emulsions is necessary for controlling/preventing emulsification processes and for improving de-emulsification technologies, hence many experimental/theoretical studies have been carried out in the last decades.[1,2] However, many publications report data obtained only with synthetic emulsions, specially formulated to support some theoretical models,[3,4] whereas studies with emulsions of native crudes are frequently aimed merely at improving some new experimental techniques.[5] As a result of preferential attention to multiple fine details, the existence of some common features of native crude oil emulsions still remain unnoticed, underinvestigated, or unexplained (e.g., it is rarely emphasized that virtually all (more than 95%) of the native crude oil emulsions formed in the oil field as well as infamous "chocolate mousses" in oil spills are of the same water-in-oil (W/O) type[6−8]). A qualitative explanation of the preference of W/O morphology is that native crude oils contain certain indigenous surfactants such as asphaltenes, resins, naphthenic acids, and oil-wet fine solids,[9] whereas, according to Bancroft's rule, the liquid in which the surfactant is soluble becomes the continuous phase. These surfactants presumably migrate to the oil−water interface and stabilize water droplets by steric and electrostatic interactions or by rigid-film formation.[1] Recently, it has been realized that interfacial material in petroleum emulsions should be regarded as a certain additional phase (third phase in the terminology of Ese et.al.[10] or D-phase as defined by Havre and Sjöblom[11]). Some compositional and structural properties of the interfacial phase have been determined by studies of specially formulated emulsions[11] and by monitoring rigid-film properties at individual water droplets.[12,13] In studies of synthetic diluted bitumen emulsions, it was observed that interfacial phases containing fine solids and asphaltenes may attain more complicated morphology by incorporating small water droplets.[14] However, in spite of continuing research, structure and function of interfacial phases in emulsions of native, as-recovered crude oils still remain under-

* Corresponding author. E-mail: physexp@gubkin.ru. URL: http://eee.gubkin.ru.

(1) Sjoblom, J. *Emulsions and Emulsion Stability*, 2nd ed.; CRC Press: New York, 2006.

(2) Sjoblom, J. *Encyclopedic Handbook of Emulsion Technology*; Marcel Dekker: New York, 2001.

(3) Zaki, N. N.; Abdel-Raouf, M. E.; Abdel-AzimA.-A. A. Propylene oxide-ethylene oxide block copolymers as demulsifiers for water-in-oil emulsions, 1. Effect of molecular weight and hydrophilic-lipophylic balance on the demulsification efficiency. *Monatsh. Chem.* **1996**, *127*, 621–629.

(4) Kang, W.; Jing, G.; Zhang, H.; Li, M.; Wu, Z. Influence of demulsifier on interfacial film between oil and water. *Colloids Surf., A* **2006**, *272*, 27–31.

(5) Pena, A. A.; Hirasaki, G. J. Enhanced characterization of oilfield emulsions via NMR diffusion and transferse relaxation experiments. *Adv. Colloid Interface Sci.* **2003**, *105*, 103–150.

(6) Berridge, S. A.; Thew, M. T.; Loriston-Clarke, A. G. The formation and stability of emulsions of water in crude petroleum and similar stocks. *J. Inst. Petrol. 54*, 333–357.

(7) Ali, M. F.; Alqam, M. H. The role of asphaltenes, resins and other solids in the stabilization of water in oil emulsions and its effects on oil production in Saudi oil fields. *Fuel* **2000**, *79*, 1309–1316.

(8) *Oil in the Sea III: Inputs, Fates, and Effects;* National Academies Press: Washington, DC, 2003.

(9) Sjoblom, J.; Aske, N.; Auflem, I. H.; Brandal, O.; Havre, T. E.; Saether, O.; Westvik, A.; Johnsen, E. E.; Kallevik, H. Our current understanding of water-in-crude oil emulsions. Recent characterisation techniques and high pressure performance. *Adv. Colloid Interface Sci.* **2003**, *100−102*, 399–473.

(10) Ese, M.-H.; Gawrys, K. L.; Spiecker, P. M.; Zhang, T.; Kilpatrick, P. K. Asphaltene and naphthenate mechanisms of emulsion stabilisation in water-in-crude oil emulsions. *Abstracts of the 225th ACS National Meeting*>, New Orleans, LA, 2003.

(11) Havre, T. E.; Sjöblom, J. Emulsion stabilization by means of combined surfactant multilayer (D-phase) and asphaltene particles. *Colloids Surf., A* **2003**, *228*, 131–142.

(12) Yeung, A.; Dabros, T.; Czarnecki, J.; Masliyah, J. On the interfacial properties of micrometre-sized water droplets in crude oil. *Proc. R. Soc. London, Ser. A* **1999**, *455*, 3709–3723.

(13) Zhang, L.; Breen, P.; Xu, Z.; Masliyah, J. Asphaltene films at a toluene/water interface. *Energy Fuels* 2007, *21*, 274–285.

10.1021/la800628j CCC: $40.75
Published on Web 06/19/2008

investigated. Our previous studies[15] have indicated that in native emulsions interfacial phases may exhibit a common small-droplet morphology and may act as stabilizing media for larger water droplets. This article gives new information with respect to the characteristics of water-in-native crude oil emulsions, and we hope that it can be used to obtain insight into underlying mechanisms of their flow behavior and stabilization mechanisms.

2. Materials and Methods

2.1. Materials. Virgin crude oil, which in the following text is referred to as oil 1 (O1), was collected directly from producing well #624 at Korobkovskoye reservoir (Volgograd, Russia) and had a density of 832 kg/m^3 and a pour point below −18 °C and contained ca. 1 wt % asphaltenes, 8 wt % resins, 2 wt % waxes, and suspended fine solids not exceeding 0.4 g/L. Oil samples were stored in the dark in air. The water in this study was a double distillate stored in air at pH ∼5.5. In emulsion studies, samples of 10 g of water + O1 oil were prepared at various weight ratios ranging from 0 to 85% (weighting accuracy 0.01 g) in standard cylindrical glass vessels. The two phases were mixed manually by vigorously shaking and upturning a vessel (with a frequency of ∼2−2.6 c^{-1}) for 10 min, which resulted in a visually homogeneous emulsion. It should be noted that some emulsion specialists may regard such a method of emulsification as too gentle compared with the use of high-speed blade mixers or ultrasound techniques in laboratory experiments.[2] However, gentle conditions of emulsification are more frequently encountered in petroleum recovery operations as well as in oil spill evolution.[6–9] Moreover, the employed manual method has ensured a reproducibility in the droplet size distribution, as will be further substantiated in part II of this article.

A type of emulsion (W/O or O/W) was inferred by a conventional drop test[16] (a drop of o/w emulsion disperses in water, whereas a drop of w/o emulsion disperses in oil). All of our emulsions, with water contents up to 85% w/w, appeared to be oil-continuous (W/O).

2.2. Shear Viscosimetry. Flow curves of emulsions (shear stresses as functions of shear rates) were determined using (1) a Brookfield DV-II+ PRO digital viscometer equipped with a concentric cylinder ULA setup (spindle diameter = 25.15 mm, gap = 1.23 mm) at shear rates from 0.06 to 100 s^{-1}; (2) a Rheotest 2.1 VEB MLW viscometer with a concentric cylinder S−S1 setup (spindle diameter = 39.2 mm, gap = 0.4 mm) at shear rates from 0.05 to 437 s^{-1}. As a standard precaution to minimize possible wall slip,[2] cylinder surfaces were pretreated with rough sandpaper. Temperature was controlled at 20 °C by a circulating water bath, typically to within 0.2 °C. When first loaded into the viscometer, each sample was presheared by applying the lowest shear rate for 3 min. The emulsion flow curves were measured as the shear rate was increased in steps. At each shear rate, the samples were equilibrated for 1 min prior to the measurement. Using this protocol, we obtained reproducible flow curves.

3. Experimental Results and Discussion

3.1. Raw Experimental Data. The measured dependencies of shear stresses on shear rates (flow curves) for emulsions of oil 1 with water volume fractions ϕ ranging from 0 to 0.825 are shown in Figures 1 and 2. Plotting flow curves on logarithmic axes facilitates the comparison of samples with parameters varying over several orders of magnitude.

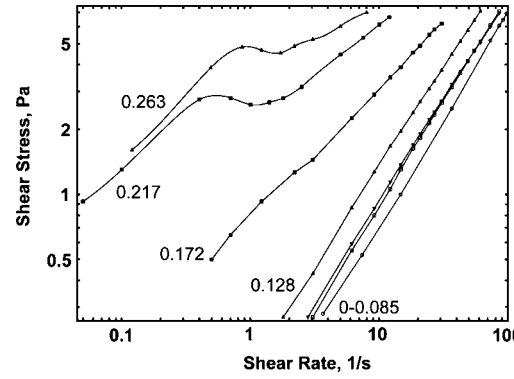

Figure 1. Flow curves for emulsions in oil 1 with low volume fractions of water (as indicated). Large-gap Brookfield viscometer.

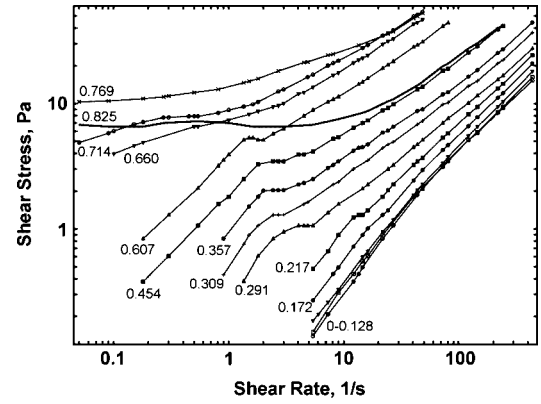

Figure 2. Flow curves for emulsions in oil 1 with a wide range of water volume fractions (as indicated). Small-gap Rheotest viscometer.

On a log−log plot, straight-line segments of the curves indicate validity ranges of a frequently employed power law (Ostwald-de Waele) flow model:[17]

$$\tau = K\dot{\gamma}^n \quad (1)$$

where n is the flow behavior index and K is the flow consistency index. Note that for $n = 1$ the model reduces to that of a Newtonian fluid, with viscosity $\eta \equiv$ K. Figures 1 and 2 show that for all emulsions with $\phi \leq 0.607$ low-shear segments of flow curves are fairly parallel (and correspond to Newtonian flow, cf. section 3.2). The apparent distortion of low-shear flow curves at $\phi =$ 0.660 and at higher water contents is due to the appearance of a noticeable yield stress (cf. Figure 3).

Flow behavior of emulsions at higher shear rates changes qualitatively around a characteristic water volume fraction ϕ^*, which depends on the viscometer's gap size (for a gap of 1.23 mm in Figure 1, $\phi^* \approx 0.14$, whereas for a gap of 0.4 mm in Figure 2, $\phi^* \approx 0.21$). For $\phi < \phi^*$, flow curves exhibit a gradual increase in shear stress with an increase in the shear rate. At water contents above ϕ^*, however, a stress plateau develops, clearly delimiting low-shear and high-shear regimes. For a given ϕ, an onset of the plateau (departure from Newtonian behavior) evidently shifts to lower shear rates as the viscometer's gap is increased. An increase in the disperse-phase volume fraction leads to systematically higher values of the critical stress at the plateau. Characteristic stress plateaus following Newtonian regimes are attributes of viscoplastic materials and are frequently observed in studies of flocculated/attractive/adhesive emul-

(14) (a) Long, Y.; Dabros, T.; Hamza, H. Structure of water/solids/asphaltenes aggregates and effect of mixing temperature on settling rate in solvent-diluted bitumen. *Fuel* 2004, *83*, 823–832. (b) Selective Solvent Deasphalting for Heavy Oil Emulsion Treatment. In *Asphaltenes, Heavy Oils, and Petroleomics*; Mullins, O. C., Sheu, E. Y., Hammami, A., Marshall, A. G., Eds.; Springer: New York, 2007, pp 511−547..

(15) Evdokimov, I. N.; Eliseev, N. Yu.; Iktisanov, V. A. Excess density in oilfield water - crude oil dispersions. *J. Colloid Interface Sci.* **2005**, *285*, 795–803.

(16) Golemanov, K.; Tcholakova, S.; Kralchevsky, P. A.; Ananthapadmanabhan, K. P.; Lips, A. Latex-particle-stabilized emulsions of anti-Bancroft type. *Langmuir* **2006**, *22*, 4968–4977.

(17) Tanner, R. I. *Engineering Rheology*, 2nd ed.; Oxford University Press: Oxford, U.K., 2000.

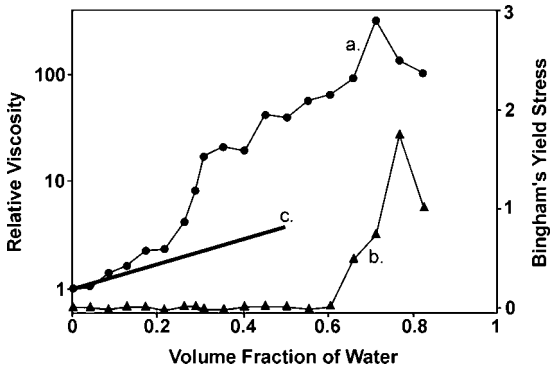

Figure 3. Effects of volume fraction of water in oil 1 on (a) low-shear relative viscosity of W/O emulsions and (b) low-shear apparent yield stress. The original flow curves were obtained in the small-gap Rheotest viscometer (cf. Figure 2). Solid line c represents the Batchelor's approximation, expressed by eq 5.

sions.[18,19] Stress plateau in emulsions are usually attributed to the breakdown of space-filling gel networks, whereas the width/slope of the plateau reflects the uniformity of the gel structure.[20] Accordingly, the data of Figure 2 suggest that the most uniform emulsion gels form at water fractions of $0.36 \leq \phi \leq 0.61$. An abrupt increase in the plateau width (distortion of gel uniformity) is observed for $\phi = 0.66$, which is fairly close to the maximally random jammed (MRJ) volume fraction of droplets,[21] $\phi_{MRJ} = 0.64$ (previously referred to as random close packing). As expected, at $\phi \geq \phi_{MRJ}$ emulsion gels become compressed,[22] and both release of strain and break-up of bonding in the gel structure commence at the lowest shear rates studied.

For water contents above $\phi = 0.74$ (hexagonal close packing of monodisperse spheres), flow curves of emulsions exhibit a new peculiar feature, namely, they intersect lower-ϕ curves at high shear rates. To highlight this behavior, the data for $\phi = 0.825$ are shown by a thick solid line in Figure 2. Visual inspection revealed that such peculiar behavior was due to the squeezing of free water from emulsion gels. It should be emphasized that even the partially dehydrated gels always remained of the W/O type and an inversion to O/W emulsions never has been observed.

Flow curves at high shear rates for all other emulsions with $\phi \leq 0.714$ exhibit qualitative similarity—fairly parallel straight-line segments on log−log plots (power law flow). There is a slight fanning of these segments due to variations of the flow behavior index from $n \approx 0.95$ for $\phi \leq 0.1$ to $n \approx 0.65$ for $\phi = 0.6-0.7$. In fact, the flow evolution of all broken gels with $0.2 \leq \phi \leq 0.7$ appears to be similar not only qualitatively but also quantitatively when analyzed in terms of excess shear parameters originating from respective gel-break points (cf. section 3.3).

In the following sections, we discuss in more detail the flow behavior of emulsions in low-shear, plateau, and high-shear ranges.

3.2. Analysis of the Low-Shear Regime. As indicated above, all low-shear segments of flow curves may be characterized by a common flow behavior index $n = 1$. To verify the validity of a true viscosity η, defined by the Newtonian model

$$\tau = \eta\dot{\gamma} \tag{2}$$

we have also approximated the discussed segments with the Bingham equation[17]

$$\tau = \tau_0 + \eta_P\dot{\gamma} \tag{3}$$

where τ_0 is an apparent yield stress and η_P is a Bingham plastic viscosity.

As illustrated by curve b in Figure 3, τ_0 acquires nonzero values only in emulsions with $\phi \geq 0.660$, hence at all lower volume fraction of water Newtonian and Bingham viscosities are virtually identical. The analysis of volume fraction effects in emulsions usually is performed in terms of the relative viscosity $\eta_{REL} = \eta/\eta_0$, where η and η_0 are viscosities of the emulsion and of the parent crude oil, respectively.[18–20] Accordingly, data set a in Figure 3 shows the effects of volume fraction of water on low-shear relative viscosities evaluated from flow curve measurements in the small-gap Rheotest viscometer (note the log scale for η_{REL}).

There are several phenomenological theories purporting the dependence of the viscosity of suspensions/emulsions on volume fraction of the disperse phase ϕ.[17] Many of these originate from the Einstein relation for spherical particles in the dilute limit:

$$\eta_{REL}(\phi) = 1 + 2.5\phi \tag{4}$$

Contributions due to hydrodynamic interactions and Brownian motion may be accounted for by a second-order term, as shown by Batchelor:[23,24]

$$\eta_{REL}(\phi) = 1 + 2.5\phi + 6.2\phi^2 \tag{5}$$

Here the factor of 6.2 is appropriate for the low-shear limit with the predominance of Brownian motion,[23] whereas in the high-shear limit, where the hydrodynamic contribution dominates, this factor reduces to 5.2.[24]

As a result of the consideration of finite particle sizes, a new crowding parameter was introduced into $\eta(\phi)$ models, namely, that of maximum packing fraction ϕ_{max}. For fairly monodisperse emulsions/suspensions, it is a common practice to identify ϕ_{max} with glass-transition volume fraction[19] $\phi_G \approx 0.58$, maximally random jammed volume fraction[21] $\phi_{MRJ} \approx 0.64$, or hcp close packing of spheres[25] $\phi_{HCP} \approx 0.74$. The most famous in this class of models is the empirical (but later verified theoretically) Krieger−Dougherty relation:[26]

$$\eta_{REL}(\phi) = \left(1 - \frac{\phi}{\phi_{max}}\right)^{-2.5\phi_{max}} \tag{6}$$

Mooney[27] also considered the crowding effect of the dispersed phase and formulated the semiempirical equation, which for spherical particles reduces to

$$\eta_{REL}(\phi) = \exp\left(\frac{2.5\phi}{1 - \phi/\phi_{max}}\right) \tag{7}$$

A comparison of experimental data in Figure 3 with the above models shows that low-shear η_{REL} in the studied emulsions

(18) Bibette, J.; Mason, T. G.; Gang, H.; Weitz, D. A. Poulin, P. Structure of adhesive emulsions. *Langmuir* **1993**, *9*, 3352–3356.
(19) Berli, C. L. A.; Quemada, D.; Parker, A. Gel transition of depletion flocculated emulsions. *Colloids Surf., A* **2003**, *215*, 201–204.
(20) Uhlherr, P. H. T.; Guo, J.; Tiu, C.; Zhang, X.-M.; Zhou, J. Z.-Q.; Fang, T.-N. The shear-induced solid-liquid transition in yield stress materials with chemically different structures. *J. Non-Newtonian Fluid Mech.* **2005**, *125*, 101–119.
(21) Mason, T. G.; Graves, S. M.; Wilking, J. N.; Lin, M. Y. Effective structure factor of osmotically deformed nanoemulsions. *J. Phys. Chem. B* **2006**, *110*, 22097–22102.
(22) Lacasse, M.-D.; Grest, G. S.; Levine, D.; Mason, T. G.; Weitz, D. A. Model for the elasticity of compressed emulsions. *Phys. Rev. Lett.* **1996**, *76*, 3448–3451.
(23) Batchelor G. K. The effect of Brownian motion on the bulk stress in a suspension of spherical particles. *J. Fluid Mech.* **1977**, *83*, 97–117.
(24) Batchelor, G. K.; Green, J. T. The determination of the bulk stress in a suspension of spherical particles to order c^2. *J. Fluid Mech.* **1972**, *56*, 401–427.
(25) de Kruif, C. G.; van Iersel, E. M. F.; Vrij, A.; Russel, W. B. Hard sphere colloidal dispersions: viscosity as a function of shear rate and volume fraction. *J. Chem. Phys.* **1985**, *83*, 4717–4725.
(26) Krieger, I. M.; Dougherty, T. J. A mechanism for non-Newtonian flow in suspensions of rigid spheres. *J. Rheol.* **1959**, *3*, 137–152.

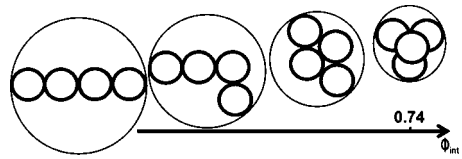

Figure 4. Variety of packing configurations in clusters of four flocculated droplets.

Table 1. Internal Volume Fraction of Water Droplets in Flocculated Clusters for Two Different Gap Viscometers (Emulsions with Volume Fraction of Water below 0.13)

model	ϕ_{max}	gap, mm	ϕ_{int}	R^2
Batchelor		1.23	0.550	0.923
		0.40	0.645	0.907
Krieger−Dougherty	0.74	1.23	0.592	0.942
		0.40	0.719	0.920
	0.64	1.23	0.602	0.944
		0.40	0.741	0.922
	0.58	1.23	0.613	0.945
		0.40	0.752	0.924
Mooney	0.74	1.23	0.654	0.948
		0.40	0.794	0.942
	0.64	1.23	0.680	0.950
		0.40	0.826	0.946
	0.58	1.23	0.699	0.952
		0.40	0.847	0.949

increases much more rapidly with ϕ than predicted by eqs 5−7. As an example, line c in Figure 3 illustrates the $\eta_{REL}(\phi)$ dependence according to Batchelor's model (eq 5). The systematic diversion of experimental and theoretical $\eta_{REL}(\phi)$ data in the dilute regime most often is ascribed to the clustering/flocculation of emulsion droplets and is interpreted in terms of (shear-dependent) effective volume fraction of clusters/flocs $\phi_{eff} > \phi$.[28,29] Higher volume fractions of the flocculated disperse phase (in our case, water) are due to the immobilization of the continuous phase (in our case, oil) inside clusters.[29] The relative amount of immobilized oil is the lowest in clusters of densely packed water droplets and increases in loosely packed (e.g., fractal) clusters. The internal volume fraction of water droplets in clusters $\phi_{int} = \phi/\phi_{eff}$ may be employed as a quantitative measure of the density of packing.[30] Figure 4 shows that there is a variety of possible ϕ_{int} already in clusters with small numbers of flocculated water droplets.

The degree of clustering in the studied emulsions was evaluated by substituting $\phi_{eff} = \phi/\phi_{int}$ instead of ϕ into eqs 5−7 and fitting the modified equations to experimental low-shear $\eta_{REL}(\phi)$ data sets with ϕ_{int} as an adjustable parameter. The fitting procedure was performed for emulsions with $\phi < 0.13$ under the assumption of negligible cluster fragmentation at small shear rates. The results of this analysis are presented in Table 1.

Sufficiently high coefficients of determination confirm the constancy of ϕ_{int} at low volume fractions of water and the reliability of systematically higher ϕ_{int} observed in the small-gap viscometer, irrespective of the employed fitting model. The respective values of ϕ_{int} suggest the presence only of densely packed clusters of water droplets under severe low-gap conditions

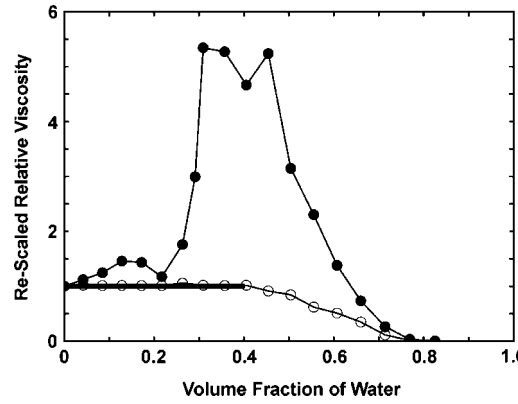

Figure 5. Experimental viscosities of W/O emulsions rescaled via dividing by the Mooney approximation. Filled symbols, low-shear regime; open symbols, high-shear regime (τ = 45 Pa). The horizontal straight line shows the ideal Mooney behavior.

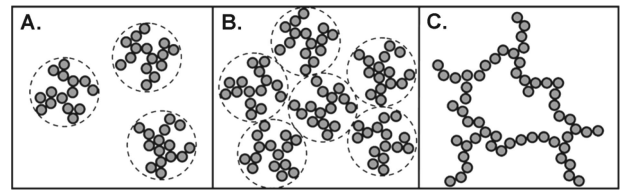

Figure 6. Apparent evolution of low-shear emulsion morphology with increasing water content. (A) Dilute clusters of flocculated water droplets. (B) Crowded clusters. (C) Space-filling emulsion gel (after ref 31).

whereas in the less constrained large-gap flow loosely packed large clusters are also retained.

At higher ϕ, cluster sizes no longer remain constant as evidenced by large departures from any of the above models (eq 5–7). To highlight this departure from smooth theoretical dependencies, we found it useful to rescale the measured emulsion viscosities via dividing the experimental $\eta_{REL}(\phi)$ data set (Figure 3) by Mooney's approximation with $\phi_{max} = 1$, namely, by $\eta_{REL} = \exp[2.5\phi/(1 - \phi)]$. The respective rescaled viscosities for low-shear conditions are shown by filled symbols in Figure 5. The horizontal straight line is the "ideal" Mooney behavior as predicted by eq 7. As described above, the systematic departure of experimental viscosities from this behavior at $\phi < 0.13-0.15$ may be attributed to the flocculation of water droplets into fairly stable/independent clusters, as indicated by the constancy of ϕ_{int}. Structural features of the disperse phase in this regime of freely moving dilute clusters are schematically illustrated in Figure 6A (after ref 31). A local maximum of rescaled viscosity at $\phi \approx 0.12$ may be attributed to a transient dynamic percolation of clusters.[32] In emulsions of nonflocculated droplets, percolation phenomena are usually observed at volume fractions of the dispersed phase close to 0.16−0.20.[33,34] In dispersions of clusters, these values should be characteristic of effective volume fractions (e.g., in the case of spherical densely packed clusters ($\phi_{int} = 0.74$), the respective phenomena may be expected at $\phi \approx 0.12-0.15$).

The second, intense, maximum in Figure 5 (at ϕ around ca. 0.4) may be identified with the glass-transition volume fraction.[19]

(27) Mooney, M. The viscosity of a concentrated suspension of spherical particles. *J. Colloid Sci.* **1951**, *6*, 162–170.
(28) Quemada, D. Rheological modeling of complex fluids. I. The concept of effective volume fraction revisited. II. Shear thickening behavior due to shear induced flocculation. *Eur. Phys. J. A* **1998**, *1*, 119127.
(29) Windhab, E. J. Fluid immobilization—a structure-related key mechanism for the viscous flow behavior of concentrated suspension systems. *Appl. Rheol.* **2000**, *10*, 134–144.
(30) Prasad, V.; Semwogerere, D.; Weeks, E. R. Confocal microscopy of colloids. *J. Phys.: Condens. Matter* **2007**, *19*, 113102.
(31) Berli, C. L. A. Rheology and phase behavior of aggregating emulsions related to droplet-droplet interactions. *Braz. J. Chem. Eng.* **2007**, *24*, 203–210.
(32) Mehta, S. K.; Bala, Kaw.; Bala, Kir. Phase behavior, structural effects, and volumetric and transport properties in nonaqueous micoremulsions. *Phys. Rev. E* **1999**, *59*, 4317–4325.
(33) *Encyclopedia of Emulsion Technology; volume 1, basic theory;* Becher, P., Ed.; Marcel Dekker: New York, 1983; *Vol. 1.*
(34) *Handbook of Microemulsion Science and Technology* Kumar, P.; K.L. Mittal, K. L., Eds.; Marcel Dekker: New York, 1999.

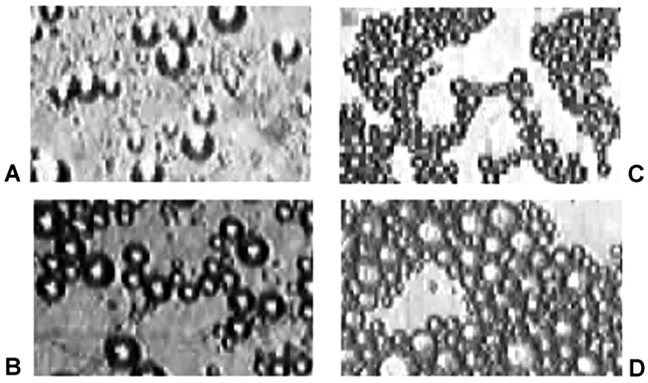

Figure 7. Microscopic images of freshly prepared W/O emulsions in oil 1 with different water contents: (A) $\phi = 0.085$, (B) $\phi = 0.263$, (C) $\phi = 0.357$, and (D) $\phi = 0.607$. The width of all rectangular areas is ~220 μm.

In nonflocculated dispersions $\phi_G \approx 0.58$, the same value should be ascribed to the effective volume fraction in the dispersion of clusters. In the above case of spherical, densely packed clusters ($\phi_{int} = 0.74$), the glass-transition phenomena may be expected at $\phi \approx 0.43$.

At the glass transition, diffusing clusters become crowded,[31,35] (i.e., they are trapped in transient cages formed by their nearest neighbors and diffusion is no longer possible; cf. Figure 6B). The result of such confinement is that clusters no longer can be regarded as individual entities. Not only intracluster but also intercluster bonds are formed between flocculating water droplet,s and the emerging disperse phase morphology is that of a 3D emulsion-gel network spanning the sample[18,31] (cf. Figure 6C). The bonds between water droplets both in the dilute clusters and in the gel morphologies apparently are weak enough to be easily broken by increasing shear rates/stresses. As an illustration, open symbols in Figure 5 show rescaled viscosities of emulsions for a shear stress of 45 Pa (cf. Figures 11 and 12). Note the absence of dilute cluster and emulsion-gel anomalies and the validity of the Mooney approximation expected for a suspension of individual nonflocculated droplets. In more detail, the break-up of droplet clusters will be discussed in section 3.3.

For the direct visualization of the above-discussed cluster/gel morphologies, we employed optical microscopy of freshly prepared W/O emulsions in oil 1. The details of these experiments and the results of droplet size, sedimentation, density, and optical analysis will be reported in part II of this article. Representative images in Figure 7 clearly show the presence of compact dilute clusters of water droplets at small ϕ (A), transient percolation into loose brunched structures (B) and spanning networks of gel-emulsion at higher volume fractions (C, D).

Note that initially-formed gel emulsions at ϕ just below and close to 0.4 are composed of visually monodisperse small droplets with a number-average diameter of ca. 10 μm. Such fairly uniform structures evidently are responsible for the strong peaking of rescaled viscosity in Figure 5. In emulsions with higher ϕ (Figure 7D), additional water is entrapped in this small-droplet gel in the form of larger-sized drops, which distorts the uniformity of the structure and reduces the rescaled viscosity at high water contents.

Our microscopy/sedimentation studies indicate that the above-discussed small-droplet gel structures play a crucial role in determining the morphological and other properties of native petroleum emulsions. These structures exhibit considerable mechanical strength and could not be broken by centrifuging at 1000*g* for 20 min. The oil-in-gel phase is remarkably different from the free-oil phase in the remaining parts of emulsion. Oil-in-gel apparently is enriched in high-MW constituents (as revealed by spectrometry and refractometry) and possesses a density that is at least 7 to 8% higher that that of the free-oil phase and of the parent crude oil. The density mismatch cannot be attributed solely to the partitioning of high-MW fractions. The emergence of some new molecular structuring in oil-in-gel is indicated by a noticeable excess density of the entire emulsion as compared to the value predicted by the ideal mixing rule.

To conclude this section, it should be emphasized that the double-peak viscosity anomaly of the type shown in Figure 5 appears to be a universal feature of native W/O petroleum emulsions, as revealed by similar rescaling of emulsion viscosities from available publications.[15,36–39] Table 2 shows the diversity of oil origins, W−O phase properties, and experimental conditions in these experiments. However, after rescaling (such as that in Figure 5), all data sets reveal qualitatively similar viscosity anomalies, peaking at water volume fractions somewhat below 0.2 and close to 0.4, as illustrated in Figure 8. (Note that for clarity of presentation some curves are shifted upward along the vertical axis, namely, curves b and h by 0.5 and curve c by 1.0). We ascribe this viscosity similarity to common cluster/gel morphologies apparently inherent to native petroleum emulsions.

For further support of the common occurrence of tight, nearly monodisperse emulsion gel structures, we may refer to our earlier observations of excess density at $\phi \approx 0.4$ in 12 different emulsions of saline reservoir brines in as-recovered native crude oils.[15] These tight emulsion gels have also been observed by direct microscopic observation of emulsions of tap water in a crude oil with properties substantially different from those of the above oil 1 (namely, $\rho = 915$ kg/m^3; 3.3 wt % asphaltenes; 24.8 wt % resins; 2.5 wt % waxes, suspended solids ≈ 0.6 mg/L).[15]

3.3. Analysis of Plateau and Higher Shear Regimes. In the discussion of Figures 1 and 2, we attributed the stress plateau in the measured flow curves to the breakdown of emulsion-gel structures. The corresponding gel break stress τ_{GB} was evaluated as the highest value of τ at the onset of departure from low-shear Newtonian behavior. Figure 9 shows the evolution of τ_{GB} in emulsions with increasing water content for two viscometers with different gap dimensions.

Extrapolations of data sets in Figure 9 to zero τ_{GB} provide characteristic volume fractions ϕ^* at which gap-spanning gels start to form (cf. also the discussion of Figures 1 and 2). Namely, for the large-gap viscometer $\phi^* = 0.142$, whereas for the small-gap one $\phi^* = 0.210$. The following linear dependence $\tau_{GB}(\phi)$ is indicative of the uniformity of increasing volume of gel domains in a decreasing volume of free oil (cf. previous section) and of the apparently negligible contribution of water droplets not incorporated into gel structures. The departure from linear behavior is observed only in the absence of free oil, for ϕ exceeding the maximally random jammed volume fraction of water droplets $\phi_{MRJ} \approx 0.64$.

One of the reviewers of this article indicated that gap size effects in Figure 9 may be interpreted on the basis of wall slipping

(35) Segrè, P. N.; Prasard, V.; Schofield, A. B.; Weitz, D. A. Glass-like kinetic arrest at the colloidal gelation transition. *Phys. Rev. Lett.* **2001**, *86*, 6042–6045.

(36) Iida, P. H.; Scheer, A. P.; Weinschutz, R.; Santos, B. M. Study of the effect of water in petroleum emulsions. In *Proc. 4 Congresso Brasileiro de P&D em Petróleo e Gás, Campinas, SP, Brazil*, 2007, Paper 2.3.0080-1.

(37) Oliveira, R. C. G.; Goncalves, M. A. L. Emulsion rheology-theory vs. field observation. In *Proc. Offshore Technology Conf. Houston, Texas*, 2005, OTC Paper 17386.

(38) Nour, A. H.; Yunus, R. M. Stability investigation of water-in-crude oil emulsion. *J. Appl. Sci.* **2006**, *6*, 2895–2900.

(39) Oliveros, K. L.; Rozhdestvenskij, E. A. Emulsion formation in the system:-Usinsk crude oil-water phase. In *Problems of Geology and Development of Fossil Fuels*, TPU Publ.: Tomsk, 2007; pp 420−421(In Russian).

Table 2. Properties of Crude Oil and Water (Brine) Phases Employed in Studies of W/O Emulsions in Various Publications[a]

crude oil origin	oil density[b], kg/m^3	oil viscosity[b], mPa·s	asphaltenes in oil, wt %	resins in oil, wt %	waxes in oil, wt %	brine/water density[b], kg/m^3	T, °C	shear rate, 1/s
a. Russia[15]	902.2	70	8.89	19.25	5.59	1154	30	<20
b. Russia[15]	905.1	76	3.03	12.65	1.96	1148	30	<20
c. Russia[15]	906.0	43	5.35	9.75	12.42	1148	30	<20
d. Brazilia[36]	868.7	10	1.09	n/a	n/a	1027	20	100
e. Brazilia[36]	898.1	51	2.33	n/a	n/a	1001	20	100
f. Brazilia[37]	n/a	28	n/a	n/a	n/a	n/a	50	50
g. Malaysia[38]	793.4	6.2	0.4	5.2	2.4	1001	30	n/a
h. Russia[39]	858.8	804	n/a	n/a	n/a	n/a	20	3

[a] The last two columns indicate conditions of reported viscosity measurements. [b] At 20 °C.

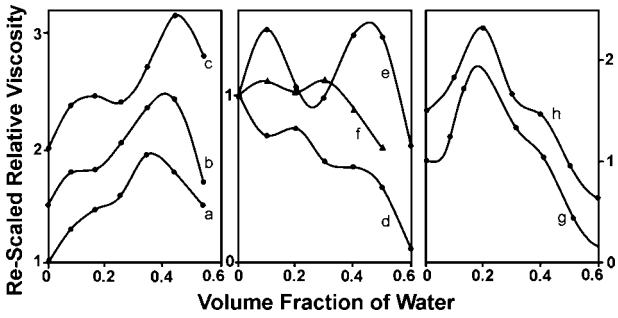

Figure 8. Apparent universality of cluster/gel morphology transformations of W/O emulsions in native crude oils from diverse geographical/geological locations (data specification in Table 2).

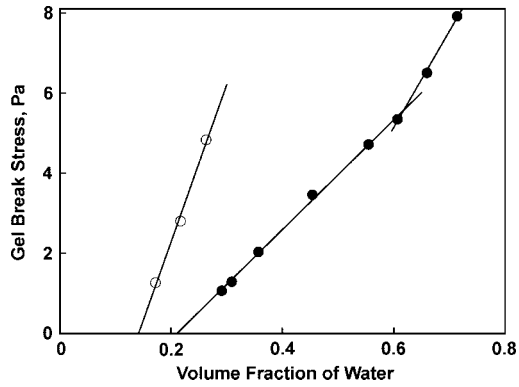

Figure 9. Gel-break stresses for W/O emulsions in oil 1. Open symbols, large-gap (1.23 mm) Brookfield viscometer. Filled symbols, small-gap (0.4 mm) Rheotest viscometer.

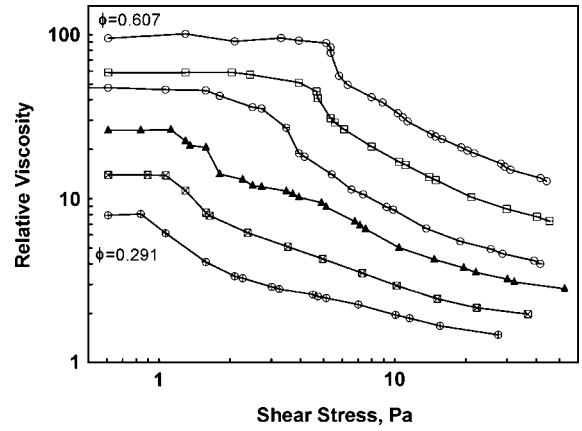

Figure 10. Viscosity vs stress for emulsions with the characteristic gel-break plateau in Figure 2.

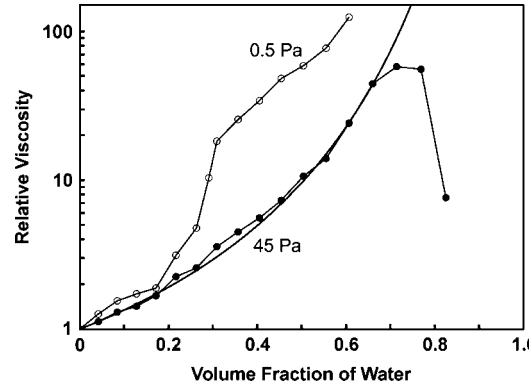

Figure 11. Effects of volume fraction of water in oil 1 on the relative viscosity of W/O emulsions at constant shear stresses of 0.5 Pa (unbroken emulsion gels) and of 45 Pa (disrupted emulsion gels). Thick line, best fit of Mooney approximation for a system of individual water droplets.

frequently observed in concentrated emulsions. Indeed, such an interpretation may be feasible. However, it should be emphasized that whereas for particle dispersions boundary surface wall slip is an experimental artifact eliminated in properly constructed rheometers,[40] for destructing gels some volume slip effects may be inherent (though gap-dependent) properties of the studied systems. In particular, gel fracture commences with crack propagation and the disentanglement of fairly large gel islands,[18,41] which in shear flow may slip with respect to each other and rotate along the shear applied, thus decreasing the measured viscosities. Moreover, the characteristic plateau at flow curves has been shown to appear at flow curves due to log-rolling movement of emulsion flocs.[42]

A common procedure in studies of viscoelastic (e.g., gel-forming) systems is to analyze structural break-up not in terms of flow curves but in terms of viscosity (i.e., shear−stress behavior).[19–21] Accordingly, in Figure 10 we present $\eta_{REL}(\tau)$ dependencies for emulsions with $0.291 < \phi < 0.607$, which exhibit a distinct gel-break plateau in Figure 2.

At shear rates less than τ_{GB}, Newtonian plateau $\eta_N = \text{const}$ is observed at all data sets in Figure 10. In this region, the local break-up rate of the gel structure by shear deformation evidently is comparable to the structural growth or recovery rate due to

(40) Barnes, H. A. A review of the slip (wall depletion) of polymer solutions, emulsions and particle suspensions in viscometers: its cause, character, and cure. *J. Non-Newton. Fluid* **1995**, *56*, 221–251.

(41) Blijdenstein, T. B. J.; Van Winden, A. J. M.; Van Vliet, T.; Van der Linden, E.; Van Aken, G. A. Serum separation and rheology of depletion- and bridging-flocculated emulsions: A comparison. *Colloids Surf., A* **2004**, *245*, 41–48.

(42) Montesi, A.; Peña, A. A.; Pasquali, M. Vorticity alignment and negative normal stresses in sheared attractive emulsions. *Phys. Rev. Lett.* **2004**, *92*, 058303

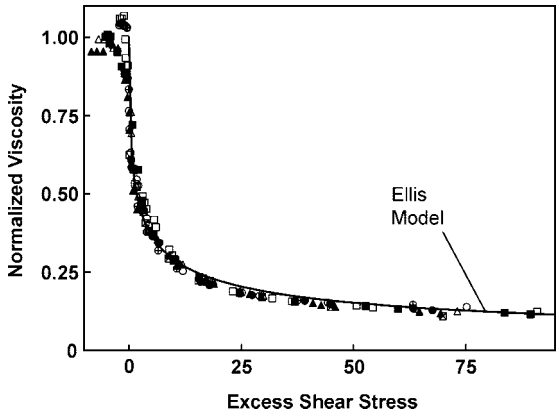

Figure 12. Single master curve for the shear-induced break-up of flocculated W/O gels in oil 1 (cf. the original data sets in Figure 11).

flocculation so that the overall resistance to flow is constant. In the intermediate shear stress region (1−3 Pa above τ_{GB}), the rate at which the gel structure is destroyed is greater than the rate of structural growth, leading to an abrupt decrease in the size of gel domains via fracturing, hence a resulting steplike decrease in viscosity. At shear stresses of 10−20 Pa above τ_{GB} and higher, there is a slower reduction in the viscosity that may be attributed to the gradual complete disruption of flocculated domains.

In support of the above interpretation, Figure 11 shows ϕ dependencies of relative emulsion viscosities for two constant values of shear stress. For $\tau = 0.5$ Pa (at the Newtonian plateau of all data sets in Figure 10), $\eta_{REL}(\phi)$ curve exhibits a prominent viscosity anomaly around $\phi \approx 0.4$ that is attributed to the presence of tight emulsion gels. This anomaly is no longer present in $\eta_{REL}(\phi)$ data for $\tau = 45$ Pa, the highest shear stress common to all of these data sets. Owing to the disruption of flocculated gels into a system of individual water droplets, the 45 Pa data may be closely approximated by the above-described Mooney model (thick line in Figure 11, $R^2 = 0.999$). As may be expected, a noticeable departure from smooth Mooney behavior is observed only for closely packed droplet morphologies ($\phi > \phi_{MRJ} \approx 0.64$) and under conditions of free-water separation at $\phi > 0.74$ (cf. discussion of Figure 2).

Further analysis of the data in Figure 10 reveals a high degree of structural similarity of gel domains in emulsions with $\phi <$ 0.64. Namely, all gel-break (shear-thinning) processes commencing at respective $\tau_{GB}(\phi)$ may be described by a single master curve when emulsion viscosity, normalized to the respective value at Newtonian plateau $\eta_{NRM} = \eta/\eta_N$, is plotted against respective excess shear stress $\tau_{EX} = \tau - \tau_{GB}$. Figure 11 shows a virtual coincidence of $\eta_{NRM}(\tau_E)$ plots for all data sets from Figure 11, except for some deviations near gel-break points.

Universal features of strong shear-thinning due to the gradual break up of flocculated aggregates in emulsions have been reported by some authors.[18–20,31] The master curves of these emulsions were interpreted through various viscosity models of colloidal dispersions, one of the most successful being the Ellis model,[43] which in the above terms may be rewritten as a two-parameter equation:

$$\eta_{NRM} = \frac{1}{1 + (\tau_{EX}/\tau_C)^{\alpha-1}} \qquad (8)$$

The solid line in Figure 11 shows that this Ellis equation provides a good approximation ($R^2 = 0.954$) of our master curve with the following parameters: $\tau_C = 1.74$ and $\alpha = 1.51$.

Note that the Ellis model is directly related to power-law approximations of flow curves (eq 1) with $\alpha - 1$ being close to flow behavior index n. Hence, the above-mentioned fanning of high-shear segments of experimental flow curves in Figure 3 may be regarded merely as a consequence of plotting data versus flow parameters originating from the zero-shear state. By transferring the origins to respective gel-break points, all segments of destructive flow should reveal similar power law behavior with $n \approx 0.51$.

4. Summary and Conclusions

In summary, flow curves of native petroleum emulsions in concentric-cylinder viscometers are composed of three distinctly different branches.

a. Low-Shear Ranges. All emulsions with water content below ca. 0.64 exhibit Newtonian behavior. The departure of Newtonian viscosities from theoretical models may be attributed to the presence of flocculated clusters of water droplets and gel structures, as revealed by viscosity anomalies as well as by direct microscopic visualization. In the small-gap viscometer,densely packed clusters are predominant, whereas under the less constrained large-gap conditions loosely packed large clusters are also retained. Characteristic tight gels composed of small droplets are responsible for the largest viscosity anomaly at water volume fractions close to 0.4. As indicated by the literature analysis, this viscosity anomaly (and, presumably, the underlying tight gel morphology) may be a universal property of native W/O petroleum emulsions.

As indicated by optical microscopy (cf. Figure 7), once formed, small-droplet gel domains apparently retain their structural integrity at higher ϕ, incorporating/stabilizing new portions of water as larger-sized droplets. The maximum hold-up of disperse water evidently is the close-packing limit of $\phi \approx 0.74$. At still higher ϕ, additional water readily emerges as a separate phase, hence there is a characteristic viscosity decrease in emulsions as a consequence of a stratified flow (W/O emulsion gel + free water; cf. Figures 3 and 11). It should be emphasized that the observed decrease in viscosity was never accompanied by the phase inversion of the closely packed emulsion gel, contrary to the conventional interpretation of the viscosity maximum as a reliable indicator of the emulsion inversion point.[36,38,39]

b. Intermediate-Shear Ranges. A gel-break plateau appears at flow curves for water contents of $\phi \geq 0.142$ in the small-gap viscometer and for $\phi \geq 0.210$ in the large-gap one. Gel-break stress τ_{GB} increases linearly with ϕ, as another indication of the uniformity of emulsion-gel morphologies. The departure from linearity commences above the maximally random jammed volume fraction of water droplets $\phi_{MRJ} \approx 0.64$.

c. High-Shear Ranges. For $\tau > \tau_{GB}$, shear-induced gel-break processes in all emulsions with $\phi < 0.74$ appear to be identical and may be described by a single master curve in terms of viscosity, which is normalized with respect to a gel-break point, versus excess shear stress above a gel-break point of $\tau_{EX} = \tau - \tau_{GB}$. In turn, this master curve exhibits a good coincidence with predictions of the power-law Ellis model.

In conclusion, the presence of domains with tight, small-droplet gel morphology may be a common feature of oil-field W/O native petroleum emulsions. Presently, apparently common mechanisms of gel formation and the common importance of $\phi \approx 0.4$ are not clear. As one of the subjects for further verification, we suggest a concept of morphology transformations in the vicinity of potential (suppressed) phase inversion. For emulsions of simple

(43) Roberts, G. P.; Barnes, H. A.; Carew, P. Modelling the flow behavior of very shear-thinning liquids. *Chem. Eng. Sci.* **2001**, *56*, 5617–5623.

fluids in the absence of specific surfactants/emulsifiers, inversion (catastrophic) at approximately equal contents of both phases is expected by spatial/thermodynamic considerations.[44,45] Most frequently, associated structural transformations proceed via small-droplet morphologies accompanying a bicontinuous state.[46,47] Our suggestion is that in native petroleum emulsions small-droplet structures also start to emerge owing to increasing confinement of the disperse phase. However, true inversion is prevented by the stabilizing action of indigenous crude oil surfactants that effectively partition into an emulsion gel. These suggestions will be supported in part II of this article by results from optical microscopy, drop size analysis, sedimentation studies, and spectrometry of oil-in-gel and free-oil subphases.

LA800628J

(44) Kralchevsky, P. A.; Ivanov, I. B.; Ananthapadmanabhan, K. P.; Lips, A. On the thermodynamics of particle-stabilized emulsions: curvature effects and catastrophic phase inversion. *Langmuir* **2005**, *21*, 50–63.

(45) Binks, B. P. Particles as surfactants - similarities and differences. *Curr. Opin. Colloid Interface Sci.* **2002**, *7*, 21–41.

(46) Allouche, J.; Tyrode, E.; Sadtler, V.; Choplin, L.; Salager, J.-L. Emulsion morphology follow-up by simultaneous in-situ conductivity and viscosity measurements during a dynamic temperature-induced translational inversion. *Proc. 3rd Int. Symp. Food Rheol. Structure*, ETH Zürich: 2003; pp 19−23.

(47) Ashby, N. P.; Binks, B. P. Pickering emulsions stabilised by Laponite clay particles. *Phys. Chem. Chem. Phys.* **2000**, *2*, 5640–5646.